

# Effects of proton pump inhibitors on reversing multidrug resistance via downregulating V-ATPases/PI3K/Akt/mTOR/HIF-1 $\alpha$ signaling pathway through TSC1/2 complex and Rheb in human gastric adenocarcinoma cells in vitro and in vivo

Min Chen,<sup>1,\*</sup> Jian Lu,<sup>1-3,\*</sup>  
Wei Wei,<sup>4,\*</sup> Ying Lv,<sup>1</sup> Xiaoqi  
Zhang,<sup>1</sup> Yuling Yao,<sup>1</sup> Lei Wang,<sup>1</sup>  
Tingsheng Ling,<sup>1,5</sup> Xiaoping  
Zou<sup>1</sup>

<sup>1</sup>Department of Gastroenterology the Affiliated Drum Tower Hospital of Nanjing University, Medical School, Nanjing 210008, People's Republic of China; <sup>2</sup>Department of Gastroenterology, the Affiliated Drum Tower Clinical Medical School of Nanjing Medical University, Nanjing 210008, People's Republic of China; <sup>3</sup>Department of Gastroenterology, the affiliated Wuxi Second Hospital of Nanjing Medical University, Wuxi 214002, People's Republic of China; <sup>4</sup>Department of Gastrointestinal Surgery, the Second Affiliated Hospital of Nanjing Medical University, Nanjing 210011, People's Republic of China; <sup>5</sup>Department of Gastroenterology, Nanjing Gaochun People's Hospital, Nanjing 211300, People's Republic of China

\*These authors contributed equally to this work

Correspondence: Xiaoping Zou; Tingsheng Ling the Affiliated Drum Tower Hospital of Nanjing University, Medical School, No 321 Zhongshan Road, Nanjing City 210008, Jiangsu Province, People's Republic of China  
Tel +86 137 7077 1661; 86 138 1304 3289  
Fax +86 25 6818 2544; 86 25 6818 2544  
Email 13770771661@163.com;  
chinalts@126.com

**Background:** Our study aimed to explore the effects of PPIs on reversing multidrug resistance (MDR) to chemotherapy in gastric cancer by inhibiting the expression of V-ATPases and the PI3K/Akt/mTOR/HIF-1 $\alpha$  signal pathway.

**Methods:** The gastric cancer cell lines SGC7901 and the multidrug resistance cell lines SGC7901/MDR were pretreated by the pantoprazole or the esomeprazole, respectively. Real-time PCR was used to determine mRNA levels, and western blotting and immunofluorescent staining analyses were employed to determine the protein expressions and intracellular distributions of the V-ATPases, PI3K, Akt, mTOR, HIF-1 $\alpha$ , P-gp and MRP1 before and after PPIs pretreatment. SGC7901/MDR cells were planted on the athymic nude mice. Then the effects of PPZ pretreatment and/or ADR were compared by determining the tumor size, tumor weight and nude mice weight.

**Results:** PPIs pretreatment could inhibit mRNA levels of V-ATPases, MDR1 and MRP1, PI3K, Akt, mTOR and HIF-1 $\alpha$ . PPIs inhibited V-ATPases and down-regulated the expressions of P-gp and MRP1. And further to block the expression of mTOR by Rapamycin could obviously inhibit the expressions of HIF-1 $\alpha$ , P-gp and MRP1 in a dose-dependent manner. Therefore, PPIs inhibited the expressions of V-ATPases and then reversed MDR of the chemotherapy in gastric cancer by inhibiting P-gp and MRP1, and it could be speculated that the mechanism might be closely related to down-regulating the PI3K/Akt/mTOR/HIF-1 $\alpha$  signaling pathway. Meanwhile, PPIs also could inhibit the expressions of TSC1/TSC2 complex and Rheb which might be involved into regulating the signaling pathway intermediately. The weight growth rate of the mice bearing tumor in the treatment group was lower than that of the nude mice in the normal group, while the weight growth rate of the mice in control group was significantly lower than that of the normal group and the treatment group, presenting a downward trend.

**Conclusion:** Therefore, PPIs inhibited the expressions of V-ATPases and then reversed MDR of the chemotherapy in gastric cancer by inhibiting P-gp and MRP1, and it could be speculated that the mechanism might be closely related to down-regulating the PI3K/Akt/mTOR/HIF-1 $\alpha$  signaling pathway, and also to inhibiting the expressions of TSC1/TSC2 complex and Rheb which might be involved into regulating the signaling pathway intermediately.

**Keywords:** gastric adenocarcinoma, V-ATPases, tumor acidity, hypoxia, proton pump inhibitors, multidrug resistance, signaling pathway

## Introduction

Gastric cancer is one of the most common digestive malignancies with lower detection rate during the early stage.<sup>1</sup> Most of patients are diagnosed after cancer has advanced rather than at early stage. Curative effects are often difficult to achieve through only surgery. Chemotherapy plays an important role in comprehensive therapy of cancer.<sup>2</sup> However, many cancers failed to respond to chemotherapy by acquiring multidrug resistance (MDR).<sup>3</sup> Although MDR had several causes, one major form of resistance to chemotherapy was closely correlated with the presence of at least three molecular “pumps” that actively transported drugs out of the cancer cells. The most prevalent of those MDR transporters were P-glycoprotein (P-gp) and the multidrug resistance protein 1 (MRP1), two members of the ATP Binding Cassette superfamily.<sup>4</sup>

Tumor microenvironment, characterized by reversed pH gradient with an acidic extracellular pH (pHe) and an alkaline intracellular pH (pHi) compared to the normal cells, closely affected tumor sensitivity to chemotherapy.<sup>5</sup> Evidence was accumulating that hypoxia and acidity were deeply involved in tumor microenvironment, resulting in cancer progression, invasiveness, metastasis, and tumor chemosensitivity. The hypoxic and acidic tumor microenvironment might conversely induce selection of tumor cells being able to survive in such an unfavorable condition.<sup>6</sup> Furthermore, a common feature of MDR cells is net decrease in the intracellular accumulation of drugs. The acid pHe will effectively impair the entry of weakly basic antitumor drugs into cancer cells since it could neutralize or sequester drugs into the acidic intracellular vesicles.<sup>7</sup>

Vacuolar H<sup>+</sup>-ATPases (V-ATPases), as a specific proton type of the cells, mainly function in the control of pHi and pHe. V-ATPases are involved in maintaining a relatively neutral pHi, luminal pH, and an acidic pHe.<sup>8</sup> Although cancer cells with low metastatic potential preferentially use Na<sup>+</sup>/H<sup>+</sup> exchangers and HCO<sub>3</sub><sup>-</sup>-based H<sup>+</sup>-transporting mechanisms, highly metastatic cells preferentially use plasma membrane V-ATPases.<sup>9</sup> The expressions of V-ATPases obviously are highly expressed in chemoresistant cancer cells and can be induced by chemotherapeutics.<sup>10</sup> Recent results showed that a molecular inhibition of V-ATPases by small interfering RNA in vivo as well as a pharmacologic inhibition through proton pump inhibitors (PPIs) led to tumor cytotoxicity and marked inhibition of human tumor growth in xenograft model.<sup>11</sup>

PPIs, mainly treating acid-related diseases, could inhibit the expressions of V-ATPases and then reverse the transmembrane pH gradient to sensitize the SGC7901 cells to the antitumor drugs, which was reflected in the downregulated

expressions of MRP1 and P-gp.<sup>11</sup> PPIs treatment reversed the pH gradient by blocking the V-ATPases-mediated H<sup>+</sup> efflux, in turn allowing anticancer drugs to penetrate and function within tumor cells.<sup>11,12</sup> However, so far, the concrete mechanism for PPIs on reversing the MDR of chemotherapy in gastric cancer was not yet known. Hence, the molecular characterization of pathways regulating chemosensitivity is a central prerequisite to improve chemotherapy.

As originally reported by Otto Warburg, most cancers are characterized by aerobic glycolysis-wasteful glycolytic conversion of glucose to lactic acid, even when sufficient oxygen is available to support efficient mitochondrial respiration.<sup>13,14</sup> In fact, an important determinant of tumor acidity is the anaerobic metabolism that allows the selection of cells able to survive in a hypoxic-anoxic environment through the upregulation of hypoxia-inducible factor 1 $\alpha$  (HIF-1 $\alpha$ ) and the adaptation of a glycolytic phenotype with generation of lactate.<sup>15</sup> HIF-1 $\alpha$ , upregulated by hypoxia, plays an important role in determining chemosensitivity focused on responsible molecular pathway.<sup>16</sup> Blocking the expression of HIF-1 $\alpha$  by siRNA in gastric cancer cells could effectively reverse MDR phenotype induced by hypoxia.<sup>15,16</sup> Although oxygen tension plays a determinant role in the process of HIF-1 $\alpha$  activation, the amplitude of this response is modulated by growth factor-dependent signaling pathways, including the Ras-Erk and phosphoinositide 3-kinase (PI 3-kinase)/AKT cascades.<sup>17</sup> Furthermore, HIF-1 $\alpha$  located the downstream of mTOR (mammalian target of rapamycin) complex 1 (mTORC1), which was regulated by the PI3K/Akt signaling pathway.<sup>18</sup> Amplified signaling through phosphoinositide 3-kinase, and its downstream target, mTORC1, enhances HIF-1-dependent gene expression in certain cancer types.<sup>19</sup> Pretreatment with the mTOR inhibitor, Rapamycin, inhibited both the accumulation of HIF-1 $\alpha$  and HIF-1-dependent transcription induced by hypoxia.<sup>20</sup>

The primary function of the TSC1-TSC2 complex is considered as a critical negative regulator of mTORC1 activation.<sup>21</sup> As with the TSC-mTOR connection, the GTP-bound Rheb regulated by the TSC1-TSC2 complex to control mTORC1 activation was identified and characterized through a combination of genetics and biochemistry.<sup>22</sup> Purified Rheb loaded with GTP, but not GDP, stimulates mTORC1's in vitro kinase activity in a dose-dependent manner, suggesting that the regulation is rather direct to a certain extent.<sup>23</sup> Nowadays, molecular characterization of signaling pathways on regulating chemosensitivity is a central prerequisite to improve cancer therapy. The PI3K/Akt/mTOR/HIF-1 $\alpha$  signaling pathway has been linked to chemosensitivity, while the underlying molecular mechanisms remain largely obscure.

Our study therefore aimed to investigate whether PPIs could improve the chemosensitivity on the gastric cancer cells via downregulating the expressions of V-ATPases, and then PI3K/Akt/mTOR/HIF-1 $\alpha$  signaling pathway by inhibiting the expressions of P-gp and MRP1. Among them, TSC1/2 complex and Rheb might be involved into regulating the signaling pathway intermediately.

## Materials and methods

### Reagents and drugs

V-ATPases 6V<sub>1</sub>A mouse polyclonal antibody was purchased from Abnova company (Taipei City, Taiwan, P.R. China). PI3 kinase p110 $\alpha$  antibody, Akt antibody, mTOR antibody, Phospho/TSC2(s933) antibody, Phospho/TSC2(Thr1462) antibody, phospho(Ser/Thr) Akt substrate antibody were purchased from Cell Signaling Technology, Inc. (Danvers, MA, USA). Hamartin (TSC1), Tuberin (TSC2), HIF-1 $\alpha$ , P-gp, MRP1, RHEB (Ras homolog enriched in brain) were purchased from Abcam PLC (Cambridge, MA, USA). Pantoprazole (PPZ) Sodium salts (Altana Pharma AG D-78467, Wesel, Germany) and Esomeprazole Sodium for Injection (AstraZeneca PLC, Cambridge, UK) were resuspended in the RPMI-1640 (pH = 6.65, in order to activate PPIs) at 1 mg/mL immediately before use. Rapamycin was purchased from LC Laboratories (Woburn, MA, USA).

### Cell lines and cell culture

Human gastric adenocarcinoma cell line, SGC7901, was kindly gifted by the Department of Oncology, the Affiliated Drum Tower Hospital of Nanjing University, Medical School. The multidrug-resistant SGC7901 cells (SGC7901/MDR) were induced by our lab with the Adriamycin and Cisplatin step by step. The average values of IC<sub>50</sub> to the Adriamycin in the SGC7901 and the SGC7901/MDR cells lines, detected by Cell Counting Kit-8 (CCK-8, MedChem Express, NJ, USA) assay, were 0.654  $\pm$  0.103 and 3.203  $\pm$  0.302  $\mu$ g/mL, respectively ( $P < 0.05$ ) (Figure 1).

Cells lines were cultured in RPMI-1640 medium (Hyclone, Thermo Fisher Scientific, Waltham, MA, USA) supplemented with 10% fetal bovine serum (Hangzhou Sijiqing Biological Engineering Materials Co., Ltd., Zhejiang, People's Republic of China) and antibiotics (100 U/mL penicillin and 100  $\mu$ g/mL streptomycin) in a humidified air with 5% CO<sub>2</sub> atmosphere at 37°C (Thermo Direct Heat CO<sub>2</sub>, Thermo Direct Inc., Garner, NC, USA). Multidrug resistant (Adriamycin and Cisplatin) SGC7901 cell strains were cultured in the Medium containing Adriamycin (800 ng/mL) maintaining their drug-resistant phenotype. The in vivo experiments strictly followed the ethical principles

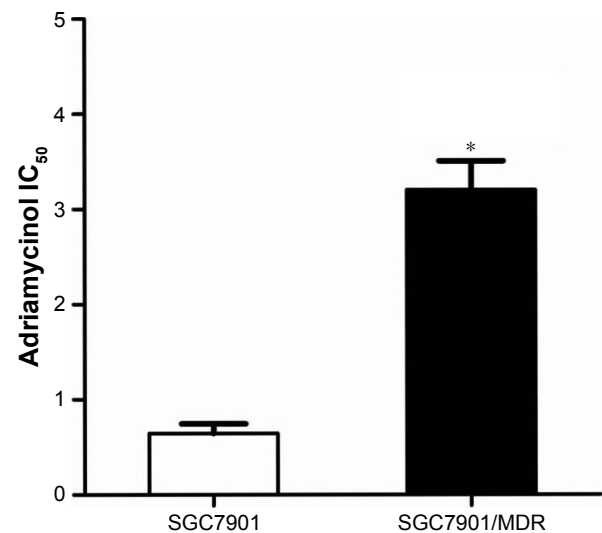


**Figure 1** The average values of IC<sub>50</sub> to the Adriamycin in the SGC7901 and the SGC7901/MDR cells lines.

**Note:** (\* $P < 0.05$ ).

and national guidelines for scientific experiments on animals. Our in vitro experiments were approved by our institutional review board and ethics committee of the Affiliated Drum Tower Hospital of Nanjing University, Medical School.

### PPIs pretreatment

The SGC7901 and SGC7901/MDR cells were treated with Esomeprazole in the medium at pH 6.65 (RPMI-1640) for 24 hours with the concentration of 0, 10, 20, 50, 80, 100  $\mu$ g/mL, respectively. SGC7901/MDR cells also were treated with PPZ for 24 hours with the same concentration gradient under the same condition.

### V-ATPases siRNA interference assay

The V-ATPases siRNA Assay kit (catalog 4390824, Ambion, Thermo Fisher Scientific) with Life Technologies (Thermo Fisher Scientific) was used according to the instructions of the manufacturer. For transfection, cells in exponential growth phase were plated in six-well plates containing antibiotic-free medium at 30% confluence and incubated overnight, then transfected with V-ATPases siRNA using lipofectamine 2000 (Invitrogen, Thermo Fisher Scientific), according to the manufacturer's protocol. The final concentration of siRNA was 50 nM. After 24 hours transfection, mediums were replaced with RPMI-1640 supplemented with 10% fetal bovine serum 24 hours. Total proteins were extracted from cells for Western blotting.

### Rapamycin inhibition assay

The SGC7901/MDR cells were seeded into six-well plates in 2 mL of standard growth medium. After an overnight culture,

the cells were washed and then transferred into low-serum (2%) medium. After starvation for 12 hours, the cells were pretreated with 20, 40, 80  $\mu\text{g}/\text{mL}$  rapamycin for 24 hours, respectively.

## RNA extraction, reverse transcription, and quantitative real-time PCR

Total RNA was extracted from cultured cells using TRIzol reagent (Sigma-Aldrich Co., St Louis, MO, USA) and reverse transcription was carried out with 1  $\mu\text{g}$  RNA in a total 20  $\mu\text{L}$  reaction volume using PrimeScript™ RT Master Mix (Takara Bio Inc., Kusatsu, Japan) according to the manufacturer's instructions as described previously.<sup>24</sup> cDNA was used as a template in Mix (Bio-Rad Laboratories Inc., Hercules, CA, USA). Quantitative real-time PCR experiments were done with the 7500 Real-time PCR system (Applied Biosystems, Thermo Fisher Scientific) by using SYBR Premix Ex Taq reagents (Takara Bio Inc.). Primers were designed and validated by Invitrogen Biotechnology Co., Ltd (Thermo Fisher Scientific). The sequences of primers used in real-time PCR are listed in Table 1. All data were normalized to the human  $\beta$ -actin. All assays were done in triplicate.

## Western blotting analysis

The SGC7901 and SGC7901/MDR Cells were gathered after various kinds of PPI pretreatments. And total protein was extracted on ice in lysate (containing 0.01% PMSF, 150 mM NaCl, 50 mM Tris (pH=8), 0.1% SDS, 0.2% EDTA, 1% Triton X-100, 1% sodium deoxycholate) supplemented with protease inhibitors (aprotinin, leupeptin, phenylmethylsulfonyl fluoride, sodium orthovanadate; Hoffman-La

Roche Ltd., Basel, Switzerland) and phosphatase inhibitors (Cell Signaling Technology, Inc.). Protein concentrations were measured by the BCA Protein Assay Kit, following the manufacturer's instructions. Equal quantities were separated by SDS-PAGE, transferred to nitrocellulose membranes using a semidry transfer system (Bio-Rad Laboratories Inc.). And probed with antibodies against V-ATPase 6V<sub>1</sub>A, PI3 kinase p110 $\alpha$ , Akt, mTOR, TSC1, TSC2, HIF-1 $\alpha$ , P-gp, MRP1, Rheb, Phospho/TSC2(Ser939), Phospho/TSC2(Thr1462), Phosphor(Ser/Thr) Akt substrate, a monoclonal mouse antibody to  $\beta$ -actin (Cell Signaling Technology, Inc.) and a monoclonal rabbit antibody to Tubulin (Bioworld Technology, Inc., St Louis Park, MN, USA) as the controls for protein loading. Anti-mouse or anti-rabbit IgG, conjugated with horseradish peroxidase (Cell Signaling Technology, Inc.) was used for secondary detection. Antibody staining was visualized by enhanced chemiluminescence (Santa Cruz Biotechnology Inc., Dallas, TX, USA). The images of Western blot products were collected and analyzed by Quantity One V4.31 (Bio-Rad Laboratories Inc.).

## Immunofluorescent staining analysis

Dispersed single cells ( $2 \times 10^5$  cells per well) were grown on  $22 \times 22 \times 1$  mm<sup>3</sup> glass cover slips (pretreated with 0.3% gelatin) in six-well culture plates. After 36–48 hours incubation and 24 hours Esomeprazole pretreatment, cells were fixed in ice-cold acetone for 10 minutes at 4°C. The cells were blocked with 10% normal goat serum (Boster Biological Technology, Pleasanton, CA, USA) for 30 minutes and probed with V-ATPase 6V<sub>1</sub>A antibodies, PI3 kinase p110 $\alpha$  antibodies, Akt antibodies, mTOR antibodies, HIF-1 $\alpha$  antibodies, and P-gp antibodies (1:100) at 4°C overnight, respectively. Alexa Fluor Dye Conjugated secondary antibodies (1:75, Alexa Fluor 488 goat anti-mouse IgG (H + L) highly cross-adsorbed), 2 mg/mL, Invitrogen Biotechnology Co., Ltd (Thermo Fisher Scientific) were used to incubate for 1 hour to be visualized under a fluorescent microscope (Imager A<sub>1</sub>, Axio, Carl Zeiss Meditec AG, Jena, Germany). DAPI (2 mg/mL, Invitrogen Biotechnology Co., Ltd, Thermo Fisher Scientific) was used to stain the nuclei.

## Effects of PPZ and/or antitumor agents on tumor growth in vivo

Solid tumor models were developed from the SGC7901/MDR cells. Forty-five male SCID immunodeficient BALB/C nude mice aged 4–6 weeks weighing 18–22 g (Model Animal Research Center of Nanjing University, People's Republic of China) were randomly divided into four groups (n = 10 each in the control, PPZ, ADR, and PPZ + ADR groups; n=5 in

**Table 1** The sequences of primers for real-time PCR

Gene	Primer sequence
<i>Actin</i>	Forward 5'-AGCGAGCATCCCCAAAGTT-3'
	Reverse 5'-GGGCACGAAGGCTCATCATT-3'
<i>V-ATPases (ATP6V0E)</i>	Forward 5'-GTCCTAACCGGGGAGTAT CA-3'
	Reverse 5'-AAAGAGAGGGTTGAGTTGGGC-3'
<i>MDR1</i>	Forward 5'-TGCGACAGGAGATAGGCTG-3'
	Reverse 5'-GCCAAAATCACAAGGGTTAGCTT-3'
<i>MRP1</i>	Forward 5'-CGGAAACCATCCACGACCCTAATCC-3'
	Reverse 5'-ACCTCCTCATTGCGATCCACCTTGG-3'
<i>PI3K (PIK3CA)</i>	Forward 5'-TTAGCTATCCACGCAGGA-3'
	Reverse 5'-CACAATAGTGTCTGTGACTC-3'
<i>AKT (AKT1)</i>	Forward 5'-CTGAGATTGTGTCAGCCCTGGA-3'
	Reverse 5'-CACAGCCCCGAAGTCTGTGATCTTA-3'
<i>mTOR</i>	Forward 5'-ATGCAGCTGTCCTGGTTCTC-3'
	Reverse 5'-AATCAGACAGGCACGAAGGG-3'
<i>HIF-1<math>\alpha</math></i>	Forward 5'-TTTTGGCAGCAACGACACAG-3'
	Reverse 5'-TGATTGAGTCAGGGTCAGC-3'

the normal group without bearing tumor), and were kept in a germ-free environment and their food, water, and bedding were autoclaved prior to use. Forty mice were subcutaneously injected with  $3 \times 10^6$  SGC7901/MDR cells resuspended in 0.2 mL of RPMI-1640 containing 10% FCS in the right scapula. Once tumors became evident (at least  $0.30 \times 0.30$  cm, approximately 10 days after the tumor cell injection), PPZ resuspended in normal saline (15 mg/mL) immediately before use was orally administered by gavage at a dose of 75 mg/kg. ADR was administered by intraperitoneal injection at a dose of 1.25 mg/kg simultaneously with PPZ oral treatment, 24 hours after PPZ treatment, or in mice that did not receive any PPZ treatment, or in mice that did only receive PPZ treatment, or in mice that even did not receive any treatment after inoculation, and or in mice that did not receive inoculation. Tumor dimensions were measured once a day with calipers and body weight were also monitored. Tumor volume was estimated by using the following formula: tumor volume ( $\text{mm}^3$ ) = length (mm)  $\times$  width<sup>2</sup> ( $\text{mm}^2$ )/2.<sup>25</sup> The relative tumor volume or body weight was expressed as the  $V_t/V_0$  or  $W_t/W_0$  index, where  $V_t$  and  $W_t$  are the tumor volume or body weight on the day of measurement and  $V_0$  and  $W_0$  are the same indices at the start of the treatment. All mice were sacrificed at the end of the experiments, within 3 weeks after the injection of the human tumor cells. Tumor specimens were fixed in 10% (v/v) neutral formalin solution for 24 hours and processed routinely by embedding in paraffin. Tissue serial sections were cut at 4  $\mu\text{m}$ . Then the TUNEL assay apoptotic cells in sections of mice tumor tissue were detected using an in situ apoptosis detection kit (KEYGEN, Nanjing City, Jiangsu Province, People's Republic of China) as instructed by the manufacturer. Cells were visualized with a light microscope (Olympus IX70, Olympus Corporation, Tokyo, Japan). The apoptotic index was calculated as follows: the apoptotic index number of apoptotic cells/total number of cells. Meanwhile, the protein expressions of V-ATPases, PI3K, AKT, mTOR, HIF-1 $\alpha$ , P-gp, and MRP1 also were determined in those tissues of bearing tumor of BALB/C nude mice. All in vivo experiments were approved by the ethical committee in the Affiliated Drum Tower Hospital of Nanjing University, Medical School.

### Statistical analysis

All data were presented as the mean  $\pm$  SD for at least three independent experiments. Statistical analysis was performed with SPSS software (version 22.0; IBM Corporation, Armonk, NY, USA). The significant differences between the two groups were then evaluated by One-way ANOVA. Statistical significance was defined as  $P < 0.05$ .

## Results

### PPIs pretreatment could inhibit mRNA levels of V-ATPases, MDR1, and MRP1

Under a medium with pH 6.65, the mRNA levels of V-ATPases, MDR1, and MRP1 significantly decreased after PPZ pretreatment (more than 20  $\mu\text{g}/\text{mL}$ ) for 24 hours on SGC7901/MDR cells when compared with those without PPZ pretreatment, which did not depend on a concentration manner (Figure 2A). As to SGC7901 cells, after PPZ pretreatment for 24 hours, the mRNA levels of MDR1 began to decrease when the concentration of PPZ was 40  $\mu\text{g}/\text{mL}$ . Meanwhile, the mRNA levels of V-ATPases and MRP1 decreased when PPZ concentration was 80  $\mu\text{g}/\text{mL}$  (Figure 2B). The amplification curve and dissolution curve are indicated in Figure 2C and D.

### PPIs pretreatment could inhibit the mRNA levels of PI3K, AKT, mTOR, and HIF-1 $\alpha$

Under a medium with pH 6.65, PPZ pretreatment (20  $\mu\text{g}/\text{mL}$ ) for 24 hours on the SGC7901/MDR cells could inhibit mRNA of PI3K significantly compared with those without PPZ pretreatment ( $P < 0.05$ ). PPZ pretreatment (40  $\mu\text{g}/\text{mL}$ ) for 24 hours on the SGC7901/MDR cells could inhibit the mRNA levels of AKT, mTOR, and HIF-1 $\alpha$  ( $P < 0.05$ ) (Figure 3A). As to the SGC7901 cells, PPZ pretreatment (40  $\mu\text{g}/\text{mL}$ ) for 24 hours could obviously inhibit the mRNA levels of PI3K than those without PPZ pretreatment ( $P < 0.05$ ). The levels of mTOR mRNA began to decrease when PPZ pretreated for 24 hours with a concentration of 60  $\mu\text{g}/\text{mL}$  ( $P < 0.01$ ). However, the levels of HIF-1 $\alpha$  decreased when the PPZ concentration was 100  $\mu\text{g}/\text{mL}$  ( $P < 0.05$ ) (Figure 3B). The amplification curve and dissolution curve are indicated in Figure 3C and D.

### PPIs inhibited V-ATPases and downregulated the expressions of P-gp and MRP1

After 24-hour treatment by Esomeprazole with different concentrations on the SGC7901/MDR cells in the medium of pH 6.65, compared with those in the control group (0  $\mu\text{g}/\text{mL}$ ), the expressions of V-ATPases and P-gp began to decrease when the concentration of Esomeprazole increased to 20  $\mu\text{g}/\text{mL}$  ( $P < 0.05$ ), and then, their expressions continued to decrease in a dose-dependent manner as the concentration of the Esomeprazole increased ( $P < 0.05$ ), when the concentration was up to 100  $\mu\text{g}/\text{mL}$ , their expressions were the lowest. Furthermore, compared to those in the

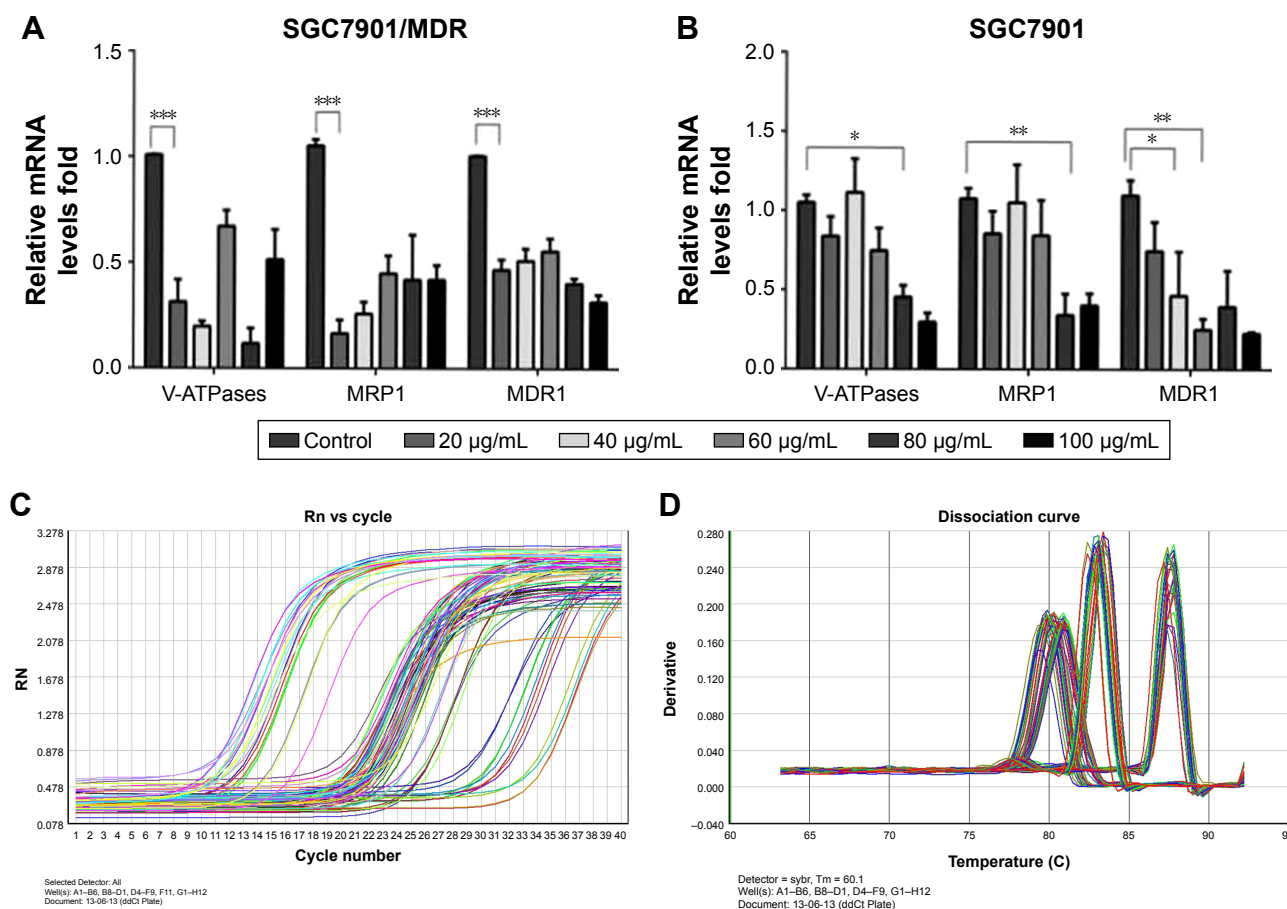


**Figure 2** PPZ pretreatment on the SGC7901 cells and SGC7901/MDR cells could inhibit mRNA levels of V-ATPases, MDR1, and MRP1.

**Notes:** (A) PPZ pretreatment could inhibit mRNA levels of V-ATPases, MDR1 and MRP1 of the SGC7901/MDR cells; (B) PPZ pretreatment could inhibit mRNA levels of V-ATPases, MDR1 and MRP1 of the SGC7901 cells; (C) Rn vs. cycle; (D) Dissociation curve. (\*\* $P < 0.005$ ; \*\* $P < 0.01$ ; \* $P < 0.05$ ).

**Abbreviation:** PPZ, pantoprazole.

control group, when the concentration of Esomeprazole was up to the 50 µg/mL, the expression of MRP1 began to decrease ( $P < 0.05$ ) and also continued to decrease in a dose-dependent manner as the concentration of the Esomeprazole increased ( $P < 0.05$ ) (Figure 4A). However, under the same conditions, after the SGC7901 cells were treated by using the same way, the expressions of V-ATPases did not decrease as the concentration of the Esomeprazole increased ( $P > 0.05$ ), and the expressions of MRP1 and P-gp were not affected either ( $P > 0.05$ ) (Figure 4B). PPZ with different concentrations also was used to treat the SGC7901/MDR cells in the same medium for 24 hours. Compared with those in the control group, the expression of V-ATPases started to decline when the PPZ concentration was up to 10 µg/mL ( $P < 0.05$ ). And with the increasing concentration of PPZ, its expression continued to decrease in a dose-dependent manner ( $P < 0.05$ ). When the PPZ concentration was up to 20 µg/mL, the expressions of the MRP1 and the P-gp began to decrease ( $P < 0.05$ ), and as the concentration of the PPZ increased, their expressions

continued to decrease dose dependently ( $P < 0.05$ ) (Figure 4C).

Subcellular localization of V-ATPases and P-gp in the SGC7901/MDR cells, before and after PPZ (100 µg/mL) pretreatment for 24 hours, were detected with the immunofluorescent staining analysis (Figure 5). And similar results were indicated in Figure 6 that subcellular localization of V-ATPases, HIF-1 $\alpha$ , and MRP1 in SGC7901/MDR cells before and after PPZ treatment (100 µg/mL) for 24 hours. It could be inferred that PPIs could change and further inhibit the subcellular localization of V-ATPases, HIF-1 $\alpha$ , P-gp, and MRP1.

### PPIs inhibited the expressions of PI3K/Akt/mTOR/HIF-1 $\alpha$ signaling pathway

SGC7901/MDR cells were dealt with Esomeprazole with different concentrations in the medium of pH 6.65 for 24 hours, compared with the control (0 µg/mL), the expressions of the PI3K and HIF-1 $\alpha$  began to decrease when the concentration of

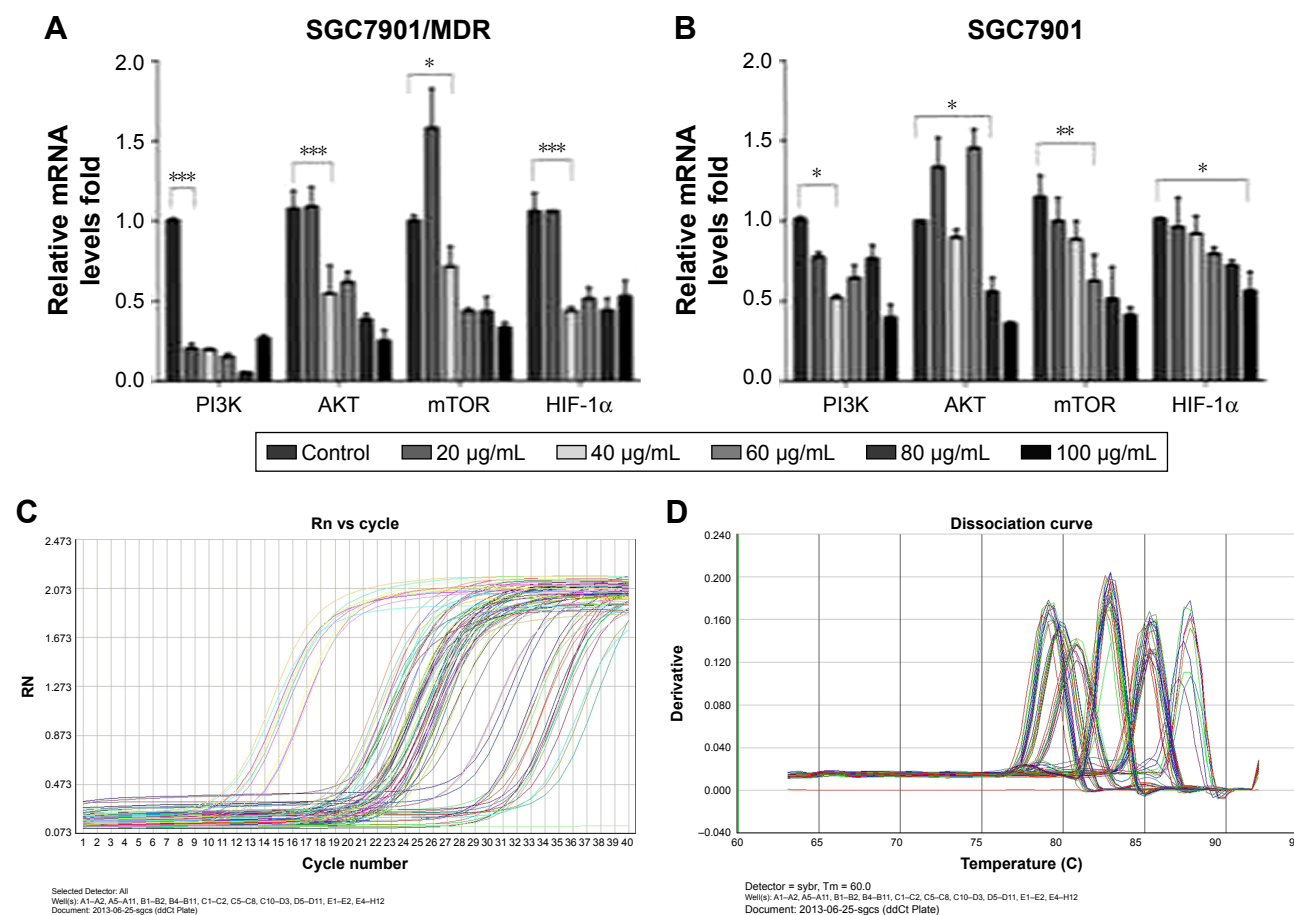


**Figure 3** PPIs pretreatment on the SGC7901 and the SGC7901/MDR cells for 24 hours could affect the mRNA levels of PI3K, AKT, mTOR, and HIF-1 $\alpha$ .

**Notes:** (A) PPZ pretreatment could inhibit mRNA levels of PI3K, AKT, mTOR and HIF-1 $\alpha$  in the SGC7901/MDR cells; (B) PPZ pretreatment could inhibit mRNA levels of PI3K, AKT, mTOR and HIF-1 $\alpha$  in the SGC7901 cells; (C) Rn vs. Cycle; (D) dissociation curve. (\*\*\*)  $P < 0.005$ ; (\*\*)  $P < 0.01$ ; (\*)  $P < 0.05$ .

**Abbreviation:** PPIs, proton pump inhibitors.

Esomeprazole was up to the 20  $\mu\text{g/mL}$  ( $P < 0.05$ ), and then, their expressions continued to be inhibited in a dose-dependent manner as the concentration of the Esomeprazole increased ( $P < 0.05$ ). When the concentration was up to 100  $\mu\text{g/mL}$ , however, their expressions were the lowest. Furthermore, compared to the control group, when the concentration of Esomeprazole went to 50  $\mu\text{g/mL}$ , the expression of Akt and mTOR began to decline ( $P < 0.05$ ) and also continued to decrease dose dependently as the Esomeprazole concentration increased ( $P < 0.05$ ) (Figure 7A).

However, under the same conditions, the expression of PI3K decreased only when the Esomeprazole concentration was up to 100  $\mu\text{g/mL}$  ( $P < 0.05$ ) by using the same way to treat the SGC7901 cells, and the expressions of the Akt, mTOR, and HIF-1 $\alpha$  were not affected ( $P > 0.05$ ) (Figure 7B).

Furthermore, the SGC7901/MDR cells were dealt with the PPZ in the same medium for 24 hours. The expressions of

PI3K, Akt, mTOR, and HIF-1 $\alpha$  started to decrease when the PPZ concentration was up to 50  $\mu\text{g/mL}$  ( $P < 0.05$ ). And as the concentration of PPZ increased, their expressions continued to decrease dose dependently ( $P < 0.05$ ) (Figure 7C).

At the same time, after Esomeprazole with different concentrations was used to treat the SGC7901/MDR cells, our study demonstrated that the expressions of TSC1 and TSC2 and Rheb started to decline when the Esomeprazole concentration up to 50  $\mu\text{g/mL}$  ( $P < 0.05$ ). And as the concentration of the Esomeprazole increased, its expression continued to decrease in a dose-dependent manner (Figure 8A). However, under the same conditions by using the same way to treat the SGC7901 cells, the expression of the TSC1 declined only when the Esomeprazole concentration was up to 100  $\mu\text{g/mL}$  ( $P < 0.05$ ), and the TSC2 expression decreased when the concentration was up to 80  $\mu\text{g/mL}$ , but as the Esomeprazole concentration increased, TSC2 expression did not decline any more. However, the Esomeprazole did not affect the

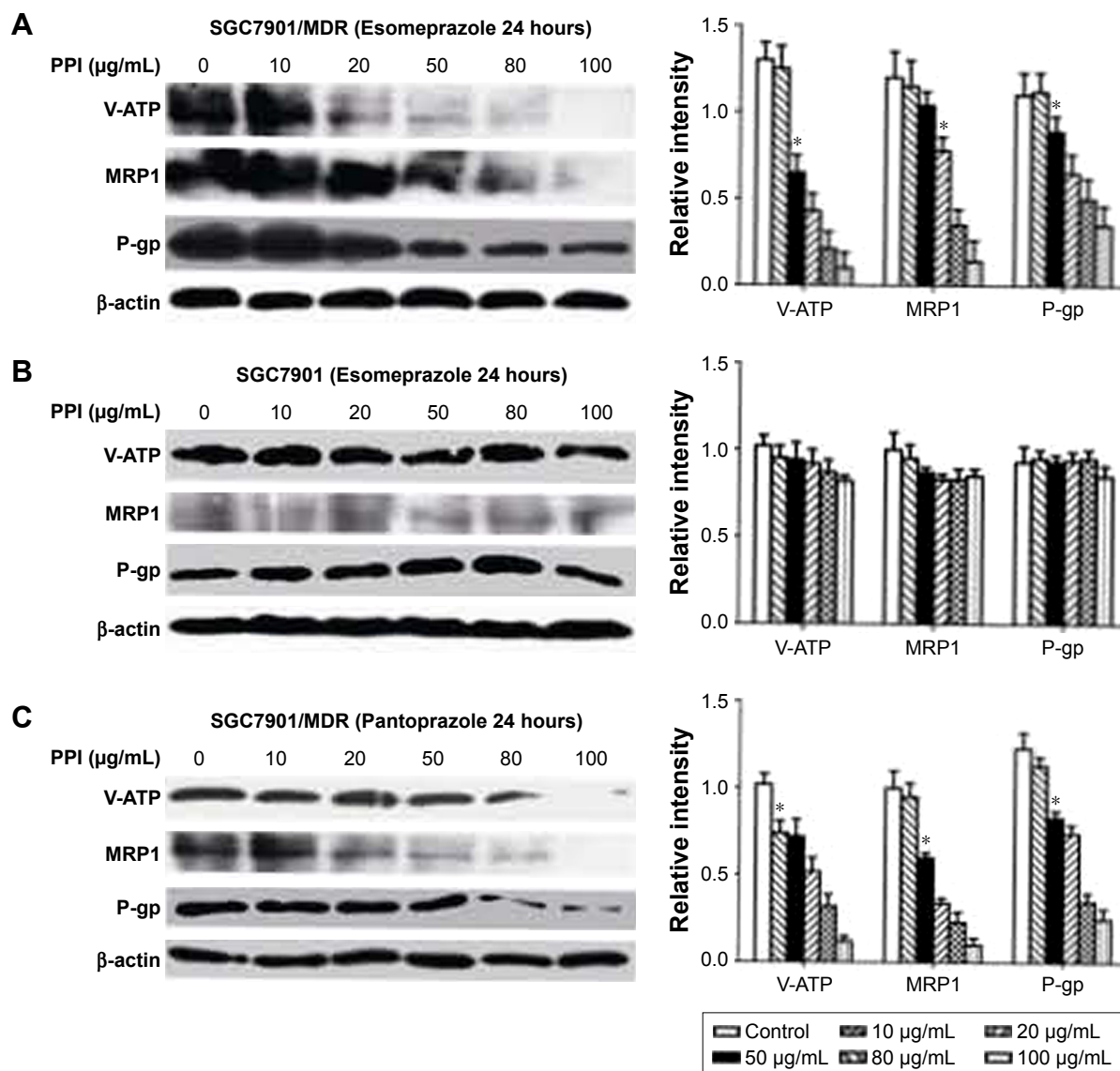


**Figure 4** Effects of PPIs pretreatment for 24 hours on the expression of V-ATPases, MRP1, and P-gp in the SGC7901/MDR and SGC7901 cell lines.

**Notes:** (A) Effects of Eesomeprazole with different concentration on the SGC7901/MDR cells in the medium of pH 6.65. The expressions of V-ATPases, MRP1, and P-gp decreased in a dose-dependent manner as the concentration of the Eesomeprazole increased. (B) Under the same conditions, using the same way to treat the SGC7901 cells, the expressions of V-ATPases did not decrease with the increasing concentration of the Eesomeprazole, and the expressions of MRP1 and P-gp were not affected, either. (C) Pantoprazole with different concentration to treat the SGC7901/MDR cells in the same medium. The expressions of V-ATPases, MRP1, and P-gp decreased dose-dependently as the concentration of Pantoprazole increased (\* $P < 0.05$  vs the control).

**Abbreviations:** PPIs, proton pump inhibitors; V-ATP, V-ATPases.

expression of the Rheb at any concentration ( $P > 0.05$ ) (Figure 8B).

After pretreatment by Eesomeprazole or PPZ for 24 hours in the SGC7901/MDR cells, the expressions of the phosphor-Ser939 and phosphor-Thr1462, which were the two phosphorylation sites of Akt to activate TSC2, also downregulated dose dependently. And the expression of the phosphor-Akt substrate decreased gradually as the concentration of the Eesomeprazole or the PPZ increased (Figure 9).

### Inhibition of the PI3K/Akt/mTOR/HIF-1 $\alpha$ signaling pathway and P-gp protein expression by V-ATPases siRNA interference

V-ATPases siRNA was used to process SGC7901/MDR cells for 24 hours, intracellular V-ATPases expression was significantly inhibited ( $P < 0.05$ ), and the intracellular protein expressions of the PI3K, Akt, mTOR, and HIF-1 $\alpha$  could be significantly inhibited ( $P < 0.05$ ), and then, the final resistance



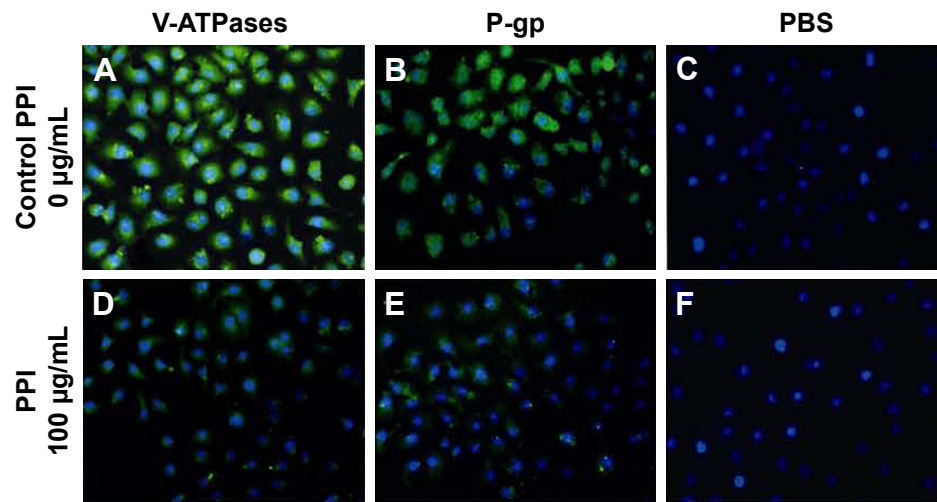


**Figure 5** Subcellular localization of V-ATPases-ATPases and P-gp in SGC7901/MDR cells before and after Pantoprazole treatment for 24 hours ( $\times 200$ ).

**Notes:** Final concentration of Pantoprazole was 100  $\mu\text{g/mL}$  (A and D). Subcellular localization of V-ATPases in SGC7901/MDR cells before and after Pantoprazole treatment (B and E). Subcellular localization of the P-gp in SGC7901/MDR cells before and after Pantoprazole treatment (C and F). Negative control: PBS buffer on behalf of the primary antibody.

protein P-gp expression decreased ( $P < 0.05$ ). However, the intracellular expressions of the TSC1 and TSC2 also were inhibited by V-ATPases siRNA ( $P < 0.05$ ) (Figure 10).

### Inhibition of mTOR expression could downregulate the intracellular HIF-1 $\alpha$ and P-gp expression

After pretreatment by Rapamycin on the SGC7901/MDR cells for 24 hours, compared with the control group,

the intracellular expression of the mTOR was significantly inhibited when the concentration of Rapamycin was up to the 20  $\mu\text{g/mL}$ , and as the concentration of Rapamycin increased, the expression of mTOR continued to decrease, and when the concentration of Rapamycin was up to 80  $\mu\text{g/mL}$ , the intracellular mTOR expression could not be detected any more. And at the same time, HIF-1 $\alpha$  and P-gp, the downstream protein of mTOR, significantly decreased when the mTOR expression was inhibited. And their intracellular

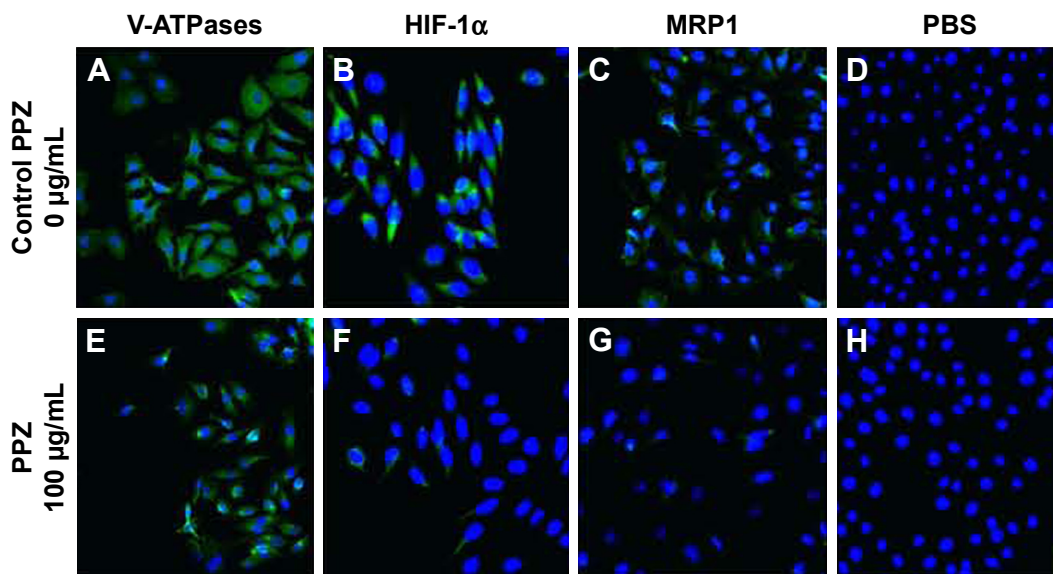


**Figure 6** Subcellular localization of V-ATPases, HIF-1 $\alpha$ , and MRP1 in SGC7901/MDR cells before and after Pantoprazole treatment for 24 hours ( $\times 200$ ).

**Notes:** Final concentration of Pantoprazole was 100  $\mu\text{g/mL}$  (A and E). Subcellular localization of V-ATPases in SGC7901/MDR cells before and after Pantoprazole treatment (B and F). Subcellular localization of the HIF-1 $\alpha$  in SGC7901/MDR cells before and after Pantoprazole treatment (C and G). Subcellular localization of MRP1 in SGC7901/MDR cells before and after Pantoprazole treatment (D and H). Negative control: PBS buffer on behalf of the primary antibody.

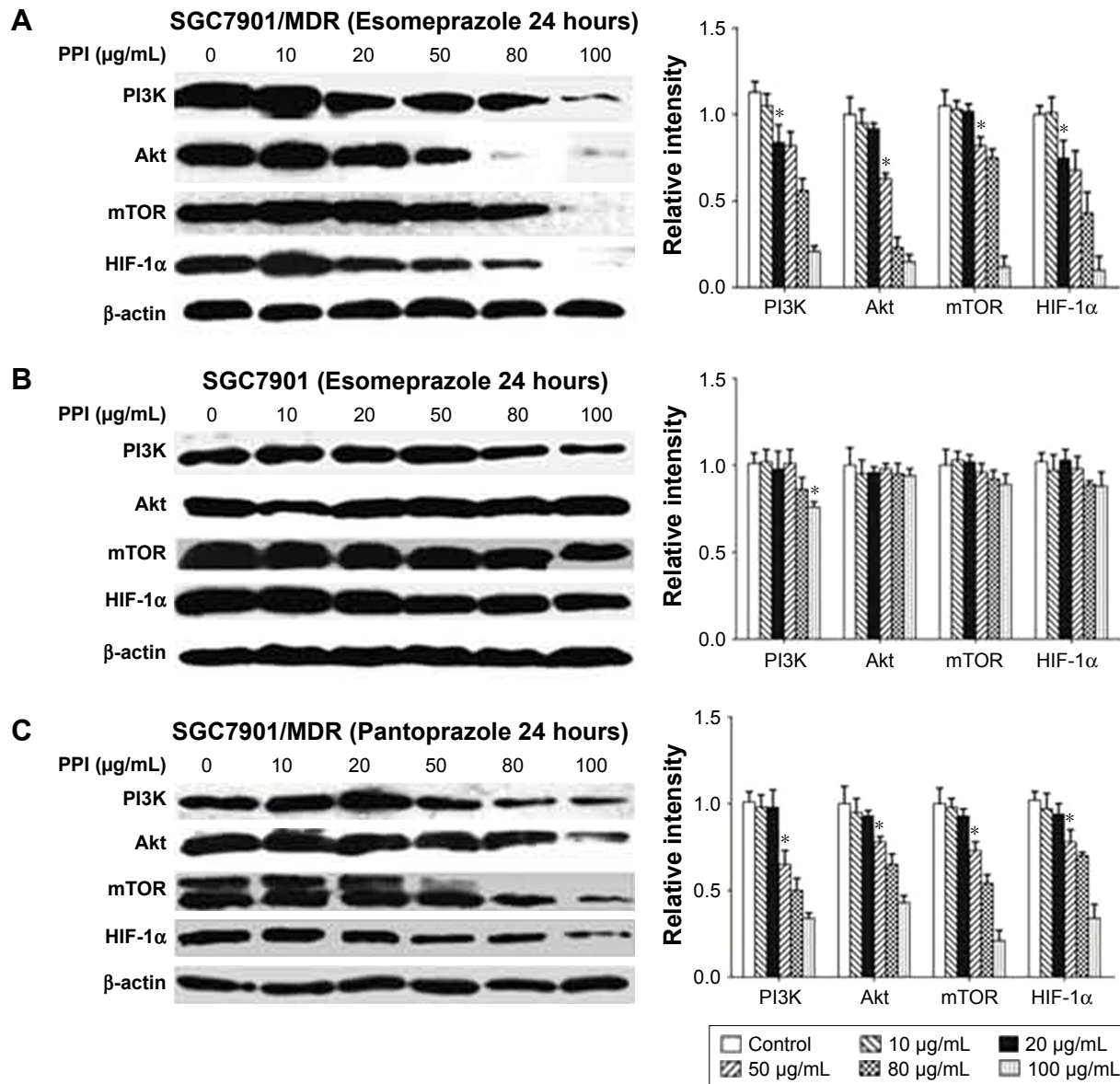


**Figure 7** Effects of PPIs pretreatment for 24 hours on the expressions of PI3K, Akt, mTOR, and HIF-1α in the SGC7901/MDR and SGC7901 cell lines.

**Notes:** (A) After Esomeprazole with different concentration to treat the SGC7901/MDR, the expressions of the PI3K, Akt, mTOR, and HIF-1α decreased in a dose-dependent manner as the concentration of the Esomeprazole increased. (B) Under the same conditions, using the same way to treat the SGC7901 cells, the expressions of the PI3K, Akt, mTOR, and HIF-1α did not decrease as the concentration of the Esomeprazole increased. (C) The SGC7901/MDR cells were dealt with the Pantoprazole in the same medium for 24 hours. The expressions of the PI3K, Akt, mTOR, and HIF-1α decreased in a dose-dependent manner as the concentration of the Pantoprazole increased (\* $P < 0.05$  vs control).

**Abbreviation:** PPI, proton pump inhibitor.

protein expressions gradually dropped with the rise of the Rapamycin's concentration, showing the remarkable concentration dependent manner (Figure 11A and B).

### PPIs on TSC1/2 complex expressions time dependently

The SGC7901/MDR cells were treated by Esomeprazole (80 μg/mL) for 3, 6, 12, 18, 24 hours, respectively. And the SGC7901/MDR cells were treated by Esomeprazole (80 μg/mL) for 15 minutes as the control. Compared with the

control, after pretreatment for 3 hours, the intracellular expression of the TSC2 began to increase ( $P < 0.05$ ), and reached the peak after 6 hours, but after 18 hours, the expression of TSC2 had no significant difference when compared with the control ( $P > 0.05$ ). For 24 hours, the TSC2 expression significantly decreased compared with the control group ( $P < 0.05$ ). Simultaneously, Esomeprazole (80 μg/mL) pretreated the SGC7901/MDR cells for 3 hours, compared to the control group, the intracellular expression of the TSC1 began to increase ( $P < 0.05$ ), and reached the peak after pretreatment

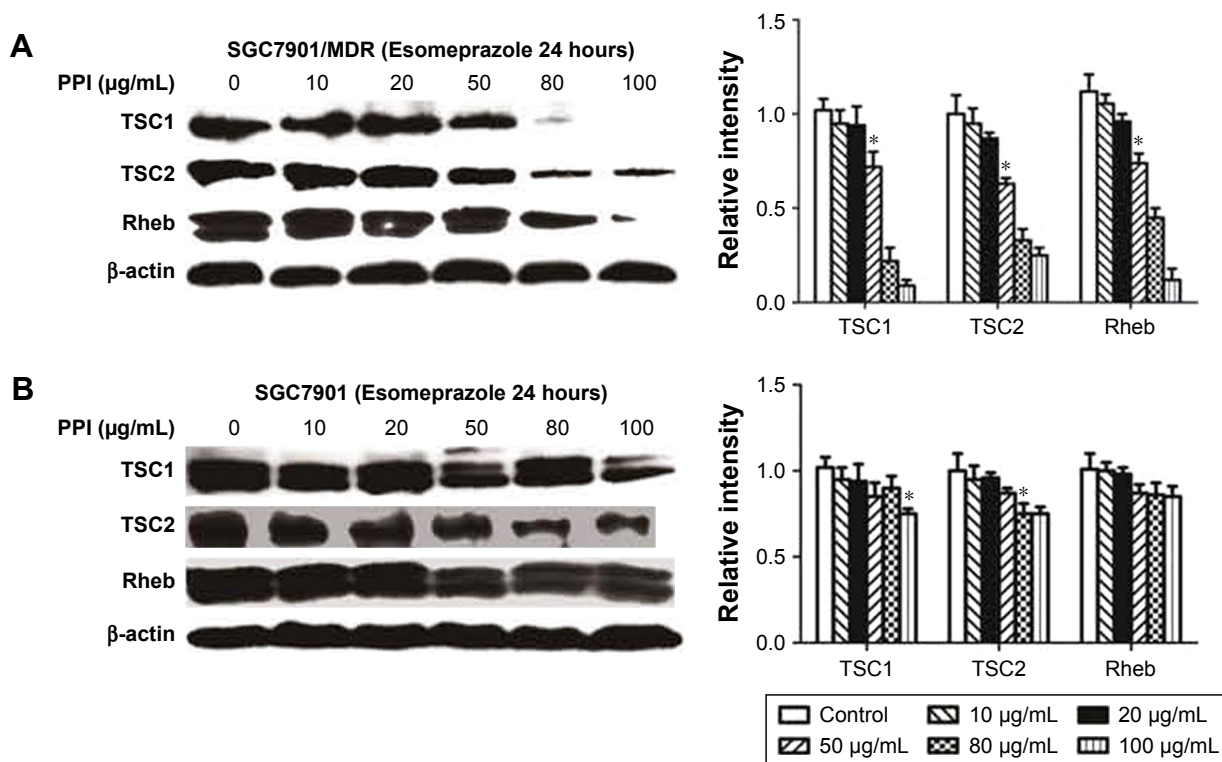


**Figure 8** Effects of PPIs pretreatment for 24 hours on the expressions of the TSC1, TSC2, and Rheb in the SGC7901/MDR and SGC7901 cell lines.  
**Notes:** (A) After Esomeprazole with different concentration to treat the SGC7901/MDR, the expressions of the TSC1, TSC2, and the Rheb decreased in a dose-dependent manner as the concentration of the Esomeprazole increased. (B) Under the same conditions, using the same way to treat the SGC7901 cells, the expression of the TSC1 declined only when the Esomeprazole concentration was up to 100 µg/mL, and the TSC2 expression decreased when the concentration was up to 80 µg/mL, but as the Esomeprazole concentration increased, the TSC2 expression did not decline any more (\* $P < 0.05$  vs the control).  
**Abbreviation:** PPI, proton pump inhibitor.

for 12 hours. And as the expression of TSC2, after 18 hours, the expression of TSC1 had no significant difference with the control group ( $P > 0.05$ ). But for 24 hours, the TSC1 expression also significantly decreased compared with the control group ( $P < 0.05$ ) (Figure 12).

### Inhibitory effects of LY294002 on protein expressions of PI3K, AKT, HIF-1 $\alpha$ , P-gp, and MRPI

LY294002 with various concentrations (including 0, 10, 20, 50 µmol/L) was used to treat the SGC7901/MDR cells

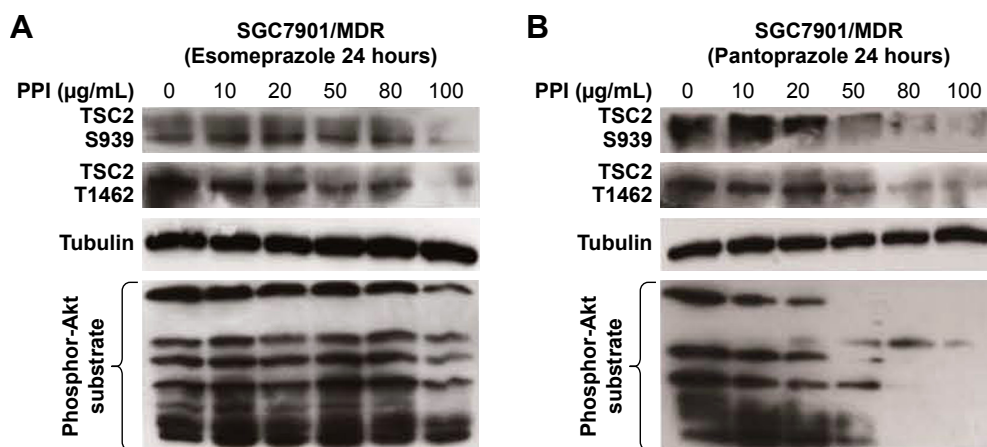


**Figure 9** Effects of PPIs pretreatment for 24 hours on the expressions of the phosphor-Ser939, phosphor-Thr1462, and phosphor-Akt substrate in the SGC7901/MDR cells.  
**Notes:** (A) Effects of the Esomeprazole on the expressions of the phosphor-Ser939, phosphor-Thr1462, and the phosphor-Akt substrate. (B) Effects of the Pantoprazole on the expressions of the phosphor-Ser939, phosphor-Thr1462, and the phosphor-Akt substrate.

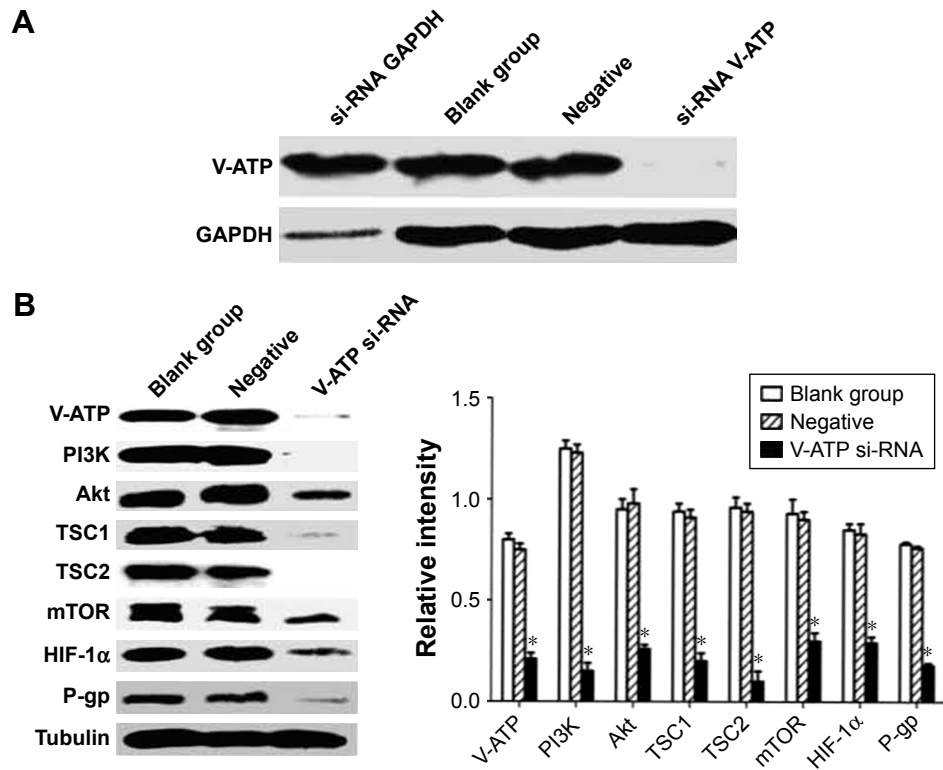


**Figure 10** Inhibitory effect on the PI3K/Akt/mTOR/HIF-1α signaling pathway in the SGC7901/MDR cell lines by interference of V-ATPases. **Notes:** (A) Western blot analysis of V-ATPases by siRNA-mediated inhibition. Interference system could effectively inhibit V-ATPases and positive control GAPDH. (B) After the expression of V-ATPases was downregulated by siRNA, the expression of the PI3K/Akt/mTOR/HIF-1α signaling pathway was significantly inhibited simultaneously. And the expression of P-gp also was downregulated (\**P* < 0.05 vs the blank group). **Abbreviation:** V-ATP, V-ATPases.

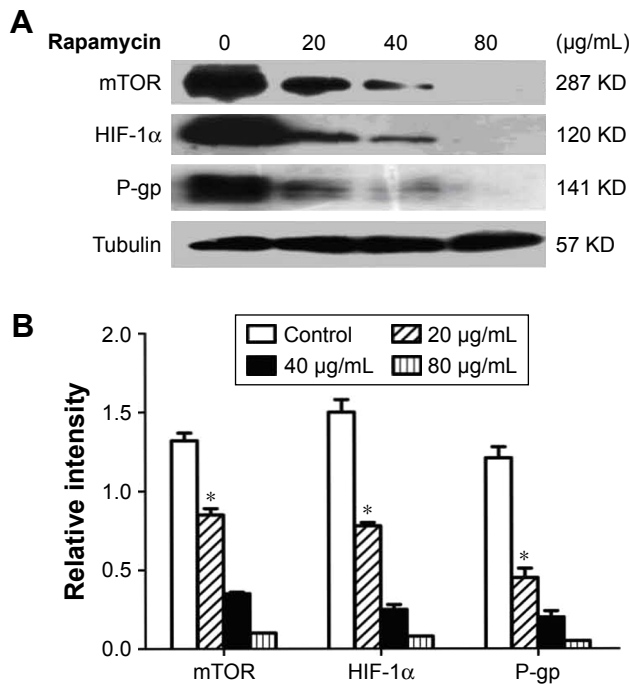


**Figure 11** Effects of the Rapamycin inhibition on the protein expressions of mTOR, HIF-1α, and P-gp in the SGC7901/MDR cells. **Notes:** (A) Inhibitory effects of Rapamycin on the protein expressions of mTOR, HIF-1α, and P-gp. (B) Relative optical density value of protein expressions of mTOR, HIF-1α, and P-gp after Rapamycin treatment (\**P* < 0.05 vs the control).

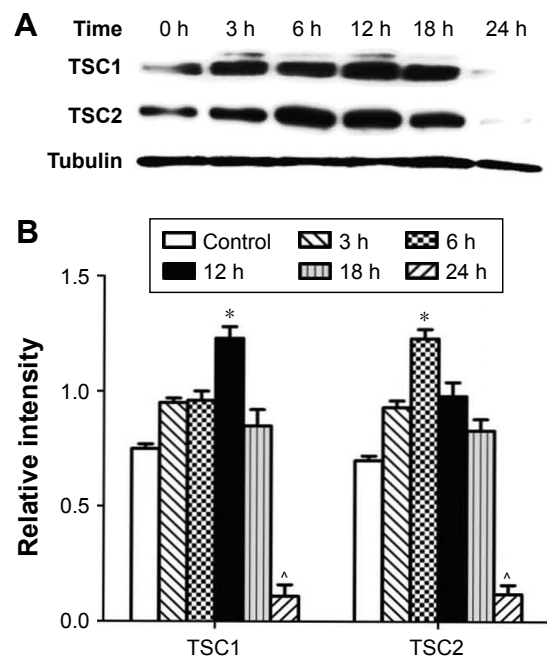


**Figure 12** Effects of PPIs on the TSC1/2 complex expressions time-dependently. **Notes:** (A) Effects of PPIs on the TSC1/2 complex expressions in a time-dependent manner. (B) Relative optical density value of TSC1/2 complex expressions after PPIs treatment. (\**P* < 0.05 vs the control, showing the expression increase, ^*P* < 0.01 vs the control, showing the expression decrease.) **Abbreviations:** PPIs, proton pump inhibitors; V-ATP, V-ATPases.

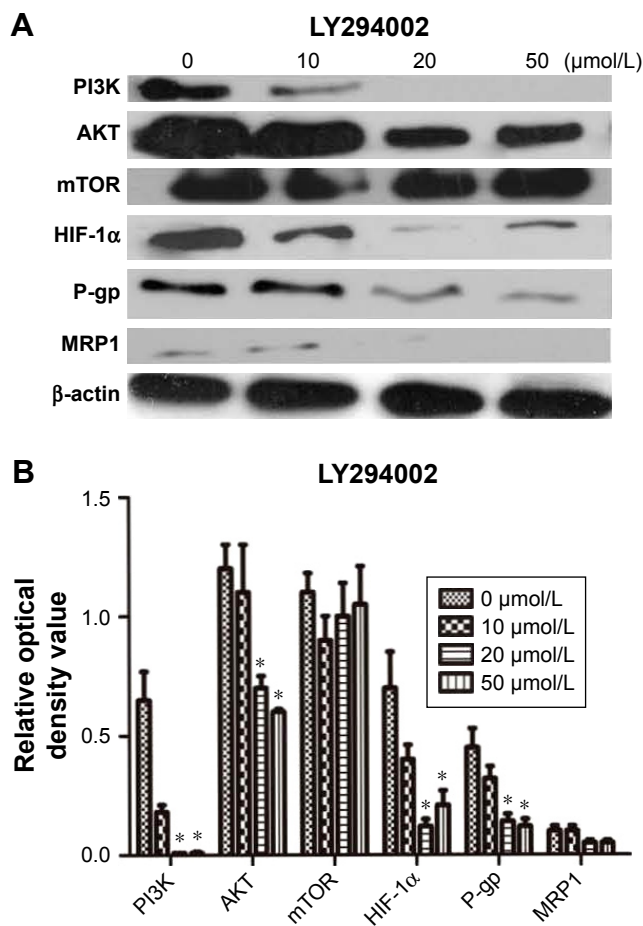


**Figure 13** Effects of LY294002 on the protein expressions of PI3K, AKT, mTOR, HIF-1 $\alpha$ , P-gp, and MRP1.

**Notes:** (A) Inhibitory effects of LY294002 on the protein expressions of PI3K, AKT, mTOR, HIF-1 $\alpha$ , P-gp, and MRP1. (B) Relative optical density value of the protein expressions of PI3K, AKT, mTOR, HIF-1 $\alpha$ , P-gp, and MRP1 after LY294002 treatment (\* $P < 0.05$  vs the control LY294002 0  $\mu\text{mol/L}$ ).

for 24 hours. Then the protein expression of PI3K was inhibited by LY294002 on a concentration-dependent manner. Then the protein expressions of PI3K, AKT, HIF-1 $\alpha$ , P-gp, and MRP1 also were significantly downregulated by LY294002 (Figure 13) ( $P < 0.05$ ), however, the protein expressions of mTOR was not affected by LY294002 ( $P > 0.05$ ).

### Effects of PPZ on sensitivity of human tumors to antitumor agents in athymic mice engrafted with the SGC7901/MDR cells in vivo

The findings of our in vivo experiments further supported our results in vitro. These mice have proved useful in assessing the in vivo efficacy of local and systemic antitumor treatments of PPZ and adrimycin (ADR). Figure 14 shows the changes of relative body weight of athymic mice, relative tumor volume of athymic mice, and the changes of relative

tumor volume in the four groups. Moreover, Figure 14 also provides the direct comparisons of tumor sizes in the four groups, in which the relative tumor volume in the PPZ + ADR group was the lowest, coincided with results in vitro. The statistical data is also summarized in Figure 14. In addition, Figure 15 shows more apoptotic cells of the tumor tissues in the PPZ + ADR group compared with the ADR group and the Ctrl group since there was a relatively higher apoptotic index in the PPZ + ADR group (Figure 15A). According to the protein expressions of bearing-tumor tissues, the expressions of PI3K, mTOR, HIF-1 $\alpha$ , and P-gp were significantly inhibited in the PPZ + ADR group, which also further supported our results in vitro. However, the expressions of V-ATPases, AKT, and MRP1 were not inhibited in the PPZ + ADR group, which were inconsistent with the data in our in vitro experiments (Figure 15B and C).

## Discussion

Intrinsic and acquired MDR are the primary causes for limited efficacy of chemotherapy in the majority of gastrointestinal malignancies, including gastric cancer.<sup>26</sup> Drug resistance represents a complex and multifactorial phenomenon related to tumor microenvironment, for example, hypoxia, acidosis and inflammation, as well as the neoplastic cell.<sup>27</sup> Tumor cell metabolism is being nowadays the object of renewed consideration for better understanding of cancer biology and therapeutic strategies.<sup>28</sup> In fact, the glucose metabolism in hypoxic conditions by the neoplasms leads to a pHi drift toward acidity. The acid microenvironment is modulated through the over-expression of H<sup>+</sup> transporters that also are involved in tumor progression, invasiveness, distant spread, and chemoresistance.<sup>29</sup> Several strategies to block/downmodulate the efficiency of these transporters are currently being investigated. Among them, PPIs have been utilized to successfully block the H<sup>+</sup> transporters in vitro and in vivo, leading to apoptotic death. Furthermore, their action seems to synergize with conventional chemotherapy protocols, leading to chemosensitization and reversal of MDR.<sup>30</sup> Evidence is demonstrated that hypoxia and acidity are involved in cancer progression and the MDR of tumor to chemotherapy. Besides, hypoxia and acidity also may contribute to the progression from benign to malignant growth. Tumor acidity, in particular, has role in resistance chemotherapy and metastatic behaviour.<sup>5,6</sup> V-ATPases play a critical role in regulating the transmembrane pH gradient. The subcellular localization of V-ATPases was mainly on the membrane of internal acidic vesicles and plasma membrane. Compared to the normal cells, in which V-ATPases only expressed on the acidic vesicle. V-ATPases

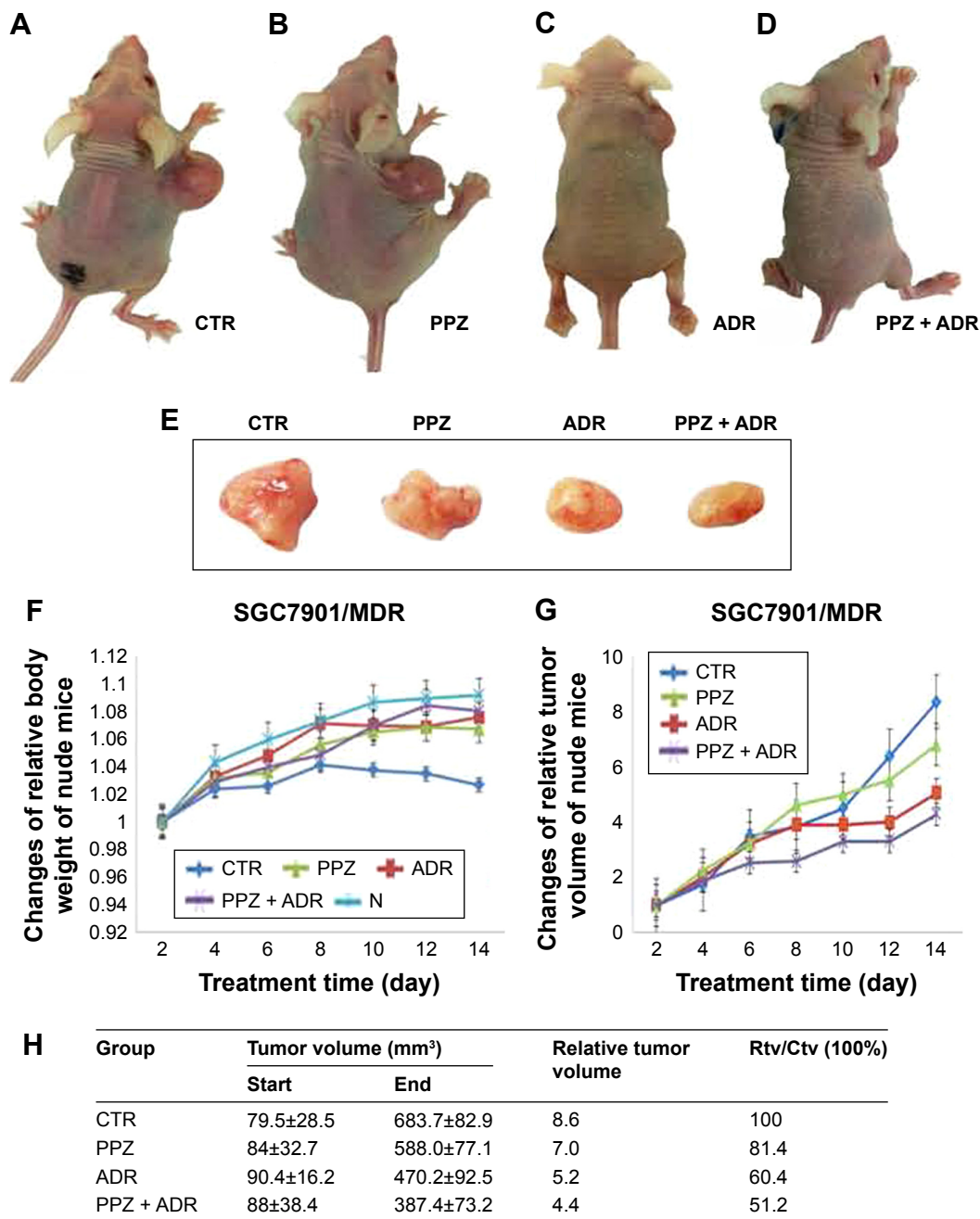


**Figure 14** Effects of PPZ on sensitivity of human tumors to antitumor agents in athymic mice engrafted with the SGC7901/MDR cells in vivo.

**Notes:** (A–E) Effects of PPZ and/or ADR on tumor size of athymic mice xenografted with the SGC7901/MDR cells. (F) Effects of PPZ and/or ADR on relative body weight of athymic mice xenografted with the SGC7901/MDR cells. (G) Effects of PPZ and/or ADR on relative tumor volume of athymic mice xenografted with the SGC7901/MDR cells. (H) Effects of PPZ and/or ADR on tumor volume and relative tumor volume of athymic mice xenografted with the SGC7901/MDR cells. PPZ resuspended in normal saline (15 mg/mL) immediately before use was orally administered by gavage at a dose of 75 mg/kg. ADR was administered by intraperitoneal injection at a dose of 1.25 mg/kg. RTV means relative tumor volume representing the ratio of tumor volume at the end and tumor volume at the beginning.

**Abbreviations:** ADR, adrimycin; PPZ, pantoprazole.

are very active in malignant cells, correlating with a high expression at both the plasma membrane and acidic vesicle level.<sup>8,9,31</sup> PPIs were the powerful tools in the treatment of human solid tumors because they could induce sensitivity to a wide range of antitumor drugs by inhibiting the expression of V-ATPases.<sup>10,11,32</sup> One major cause of resistance to

chemotherapy has been correlated with the presence of the “pumps” that actively transport drugs out of the cell. The most prevalent transporters of MDR are p-gp and MRP1.<sup>33</sup> Our studies demonstrated that both PPZ and Esomeprazole could inhibit the intracellular expressions of the V-ATPases with the simultaneous suppression of expressions of P-gp

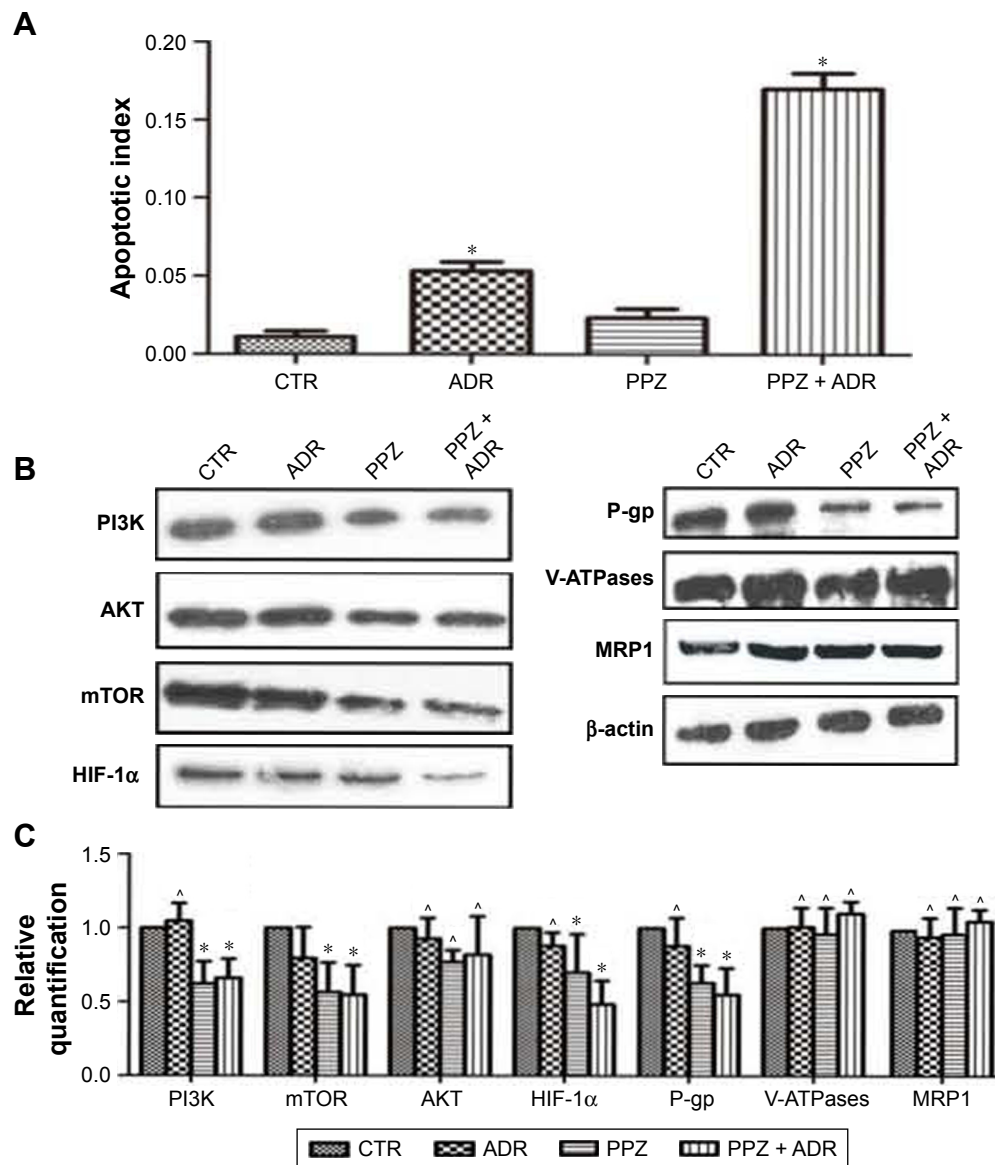


**Figure 15** Effects of PPZ on the PI3K/AKT/mTOR/HIF-1 $\alpha$  signaling pathway in the bearing-tumor tissues of athymic mice.

**Notes:** (A) Comparison of apoptotic index in the four groups by using PPZ and/or ADR. (B) Effects of PPZ and/or ADR on protein expressions of PI3K, AKT, mTOR, HIF-1 $\alpha$ , P-gp, V-ATPases, and MRP1 in the bearing-tumor tissues of athymic mice. (C) Effects of PPZ and/or ADR on the relative quantification of protein expressions of PI3K, AKT, mTOR, HIF-1 $\alpha$ , P-gp, V-ATPases, and MRP1 in the bearing-tumor tissues of athymic mice. \* $P < 0.05$ ;  $^{\Delta}P > 0.05$ .

and MRP1 in a dose-dependent manner. And the subcellular localization of the V-ATPases and P-gp in SGC7901/MDR cells differed greatly before and after PPIs pretreatment. Furthermore, downregulating the intracellular expression of V-ATPases by siRNA interference also could inhibit the expression of P-gp. These results implied that PPIs could inhibit the expression of V-ATPases, reverse the intracellular and extracellular pH gradients, and then downregulate the expression of the resistance protein so as to improve the chemosensitivity and reverse MDR. However, so far, the exactly intracellular signal mechanism of PPIs to reverse the drug resistance has been not yet known.

Evidences suggested that the acid pHe could activate the PI3K/AKT signaling pathway and could significantly enhance phosphorylation of AKT.<sup>34</sup> Many of these cellular growth and metabolism involve signaling through the PI3K/AKT/mammalian target of rapamycin pathway (mTOR pathway).<sup>35</sup> In particular, the mTOR pathway appears to play a central role in the development of multiple cancers. Although often called “a master regulator”, mTOR is one signaling target in an intricate signaling cascade that controls cell growth and angiogenesis in both normal and cancerous conditions. Other important factors in this pathway include upstream activators such as PI3K and AKT, negative regulators such as the

tuberous sclerosis complex1/2 (TSC1/2),<sup>36</sup> and downstream effectors such as the transcription factor hypoxia-inducible factor 1 $\alpha$  (HIF-1 $\alpha$ ). Evidence demonstrated that amplified signaling through phosphoinositide 3-kinase, in turn, phosphorylating and activating Akt and its downstream target, mTOR, enhances HIF-1-dependent gene expression in certain cell types; and rapamycin, as the specific mTOR inhibitor, inhibits both the accumulation of HIF-1 $\alpha$ - and HIF-1-dependent transcription induced by hypoxia.<sup>37</sup> HIF-1 constitutes a pivotal regulator of cellular adaptation to hypoxia and has been implicated in MDR.<sup>38,39</sup> HIF-1 $\alpha$  is centrally involved in multiple aspects of tumorigenesis including tumor cell proliferation, angiogenesis, metastasis, as well as the response to chemotherapy and radiotherapy. HIF-1 $\alpha$  is overexpressed in a vast number of solid tumors, and tumorous HIF-1 $\alpha$  expression is often associated with poor prognosis.<sup>40</sup> Therefore, the PI3K/Akt/mTOR/HIF-1 $\alpha$  signaling pathway has been reported closely to be linked to chemosensitivity. Our studies clarified that PPIs could inhibit the intracellular protein expressions of PI3K/AKT/mTOR/HIF-1 $\alpha$  signaling pathway and also could decrease the phosphorylation of AKT substrate. AKT was the first kinase demonstrated to directly phosphorylate the TSC1-TSC2 complex in cells in response to growth factors. And the main sites of the human TSC2 to be phosphorylated by AKT were Ser939 and Thr1462.<sup>41-43</sup> And after the pretreatment by PPIs, the phosphorylations of the two sites, Ser939 and Thr1462, were significantly inhibited as the concentration of PPIs in the SGC7901/MDR cells increased. After the V-ATPases were knocked down by the siRNA in the SGC7901/MDR cells, the intracellular protein expressions of PI3K/Akt/mTOR/HIF-1 $\alpha$  signaling pathway also were significantly inhibited, suggesting that PPIs could inhibit the PI3K/Akt/mTOR/HIF-1 $\alpha$  signaling pathway by the way of downregulating the expression of V-ATPases.

TSC1 and TSC2 are the tumor-suppressor genes mutated in the tumor syndrome TSC (tuberous sclerosis complex). The TSC1-TSC2 (hamartin-tuberin) complex, through its GAP (GTPase-activating protein) activity toward the small G-protein Rheb (Ras homologue enriched in brain), is a critical negative regulator of mTORC1 (mammalian target of rapamycin complex 1).<sup>44</sup> PPIs could inhibit the expression of Rheb dose dependently, and simultaneously the expression of the TSC1-TSC2 complex increased significantly compared with the control group. So, PPIs could inhibit the expression of mTOR through the TSC1-TSC2 complex signaling pathway. However, our results showed that after 24-hour pretreatment by PPIs on the SGC7901/MDR cells, the V-ATPases siRNA interference could inhibit

the expressions of TSC1-TSC2 complex, and at the same time, the intracellular expression of mTOR also decreased with the V-ATPases, suggesting negative feedback involving various mechanisms of activation. The conclusion was confirmed through the inhibitory effects of PPIs on TSC1/2 complex expressions not only dose dependently but also time dependently. The TSC1/2 complex expressions kept on increasing from the beginning and then decreasing while the underlying molecular mechanisms remained largely elusive. Also, PPIs treatment inhibited the expressions of Rheb dose dependently. Therefore, we speculated that TSC1/2 complex and Rheb might be greatly involved in the effects of PPIs on regulating the PI3K/AKT/mTOR/HIF-1 $\alpha$  signaling pathway.

At this time, we found that downregulating the expression of V-ATPases could inhibit the expressions of PI3K/Akt/mTOR/HIF-1 $\alpha$  signaling pathway as well as of P-gp and MRP1. Meanwhile, siRNA interference on the expression of V-ATPases also could downregulate the expressions of TSC1/2 complex. But it was not yet clarified whether the PPIs inhibited the P-gp and MRP1 was via the PI3K/Akt/mTOR/HIF-1 $\alpha$  signaling pathway or not. mTORC1 is strongly sensitive to inhibition by the naturally occurring compound rapamycin. And the mTOR protein function has relied heavily on the use of Rapamycin and are therefore probably specific to mTORC1, which was located the downstream of PI3K/Akt, and upstream of HIF-1 $\alpha$ . Our data showed that mTOR protein expression, as well as the HIF-1 $\alpha$  and P-gp, decreased in a dose-dependent manner as the concentration of the rapamycin increased. Therefore, we predicted that P-gp might locate the downstream of mTOR. Evidence had demonstrated that HIF-1 $\alpha$  determined gastric cancer chemosensitivity via modulation of p53 and NF- $\kappa$ B. However, the relationship between drug-resistance proteins such as P-gp or MRP1 and HIF-1 $\alpha$  was not yet been clarified. The underlying molecular mechanisms as well as the role of HIF-1 $\alpha$  for MDR under hypoxic conditions remain largely elusive.

## Conclusion

PPI inhibits the expression of V-ATPases, downregulates the MDR so as to sensitize the SGC7901/MDR cells to the antitumor drugs. Our study added some important information on the preclinical setting-up for the use of PPIs in the treatment of a poorly treatable tumor such as human gastric cancer. And simultaneously, the PI3K/Akt/mTOR/HIF-1 $\alpha$  signaling pathway has been linked to chemosensitivity. Downregulation of V-ATPases expression by PPIs could



inhibit the PI3K/AKT/mTOR/HIF-1 $\alpha$  signaling pathway to decrease the expressions of P-gp and MRP1 and facilitate the chemosensitivity of SGC7901/MDR to the antitumor drugs. Among them, PPIs might also downregulate TSC1/TSC2 complex and Rheb which might be involved into the regulation mechanism of PI3k/AKT/mTOR/HIF-1 $\alpha$  signaling pathway. However, the possible relevant signaling pathway of PPIs was involved into enhancing the chemosensitivity and reversing MDR also needs further research in vivo.

## Conclusion

PPIs could reverse MDR via downregulating V-ATPases/PI3K/Akt/mTOR/HIF-1 $\alpha$  signaling pathway through TSC1/2 complex and Rheb in human gastric adenocarcinoma cells in vitro and in vivo.

## Data sharing statement

All the data involved in our study are available.

## Acknowledgment

The study was supported by the Outstanding Youth Project of Nanjing Medical Scientific and Technological Development Project of Nanjing City (grant no JQX14005).

## Author contributions

All authors made substantial contributions to conception and design, acquisition of data, or analysis and interpretation of data; took part in drafting the article or revising it critically for important intellectual content; gave final approval of the version to be published; and agree to be accountable for all aspects of the work.

## Disclosure

The authors report no conflicts of interest in this work.

## References

- Cheng XJ, Lin JC, Tu SP. Etiology and prevention of gastric cancer. *Gastrointest Tumors*. 2016;3(1):25–36.
- Cunningham D, Allum WH, Stenning SP, et al; MAGIC Trial Participants. Perioperative chemotherapy versus surgery alone for resectable gastroesophageal cancer. *N Engl J Med*. 2006;355(1):11–20.
- Zhao YY, Yu L, Liu BL, He XJ, Zhang BY. Downregulation of P-gp, Ras and p-ERK1/2 contributes to the arsenic trioxide-induced reduction in drug resistance towards doxorubicin in gastric cancer cell lines. *Mol Med Rep*. 2015;12(5):7335–7343.
- Aller SG, Yu J, Ward A, et al. Structure of P-glycoprotein reveals a molecular basis for poly-specific drug binding. *Science*. 2009;323(5922):1718–1722.
- Tarrado-Castellarnau M, de Atauri P, Cascante M. Oncogenic regulation of tumor metabolic reprogramming. *Oncotarget*. 2016;7(38):62726–62753.
- Koltai T. Cancer: fundamentals behind pH targeting and the double-edged approach. *Onco Targets Ther*. 2016;9:6343–6360. eCollection 2016.
- Achour O, Ashraf Y, Bridiau N, et al. Alteration of cathepsin D trafficking induced by hypoxia and extracellular acidification in MCF-7 breast cancer cells. *Biochimie*. 2016;121:123–130.
- Smith GA, Howell GJ, Phillips C, Muench SP, Ponnambalam S, Harrison MA. Extracellular and luminal pH regulation by vacuolar H<sup>+</sup>-ATPase isoform expression and targeting to the plasma membrane and endosomes. *J Biol Chem*. 2016;291(16):8500–8515.
- Cotter K, Stransky L, McGuire C, Forgac M. Recent insights into the structure, regulation, and function of the V-ATPases. *Trends Biochem Sci*. 2015;40(10):611–622.
- Luciani F, Spada M, De Milito A, et al. Effect of proton pump inhibitor pretreatment on resistance of solid tumors to cytotoxic drugs. *J Natl Cancer Inst*. 2004;96(22):1702–1713.
- Chen M, Huang SL, Zhang XQ, et al. Reversal effects of pantoprazole on multidrug resistance in human gastric adenocarcinoma cells by down-regulating the V-ATPases/mTOR/HIF-1 $\alpha$ /P-gp and MRP1 signaling pathway in vitro and in vivo. *J Cell Biochem*. 2012;113(7):2474–2487.
- Chen M, Zou X, Luo H, et al. Effects and mechanisms of proton pump inhibitors as a novel chemosensitizer on human gastric adenocarcinoma (SGC7901) cells. *Cell Biol Int*. 2009;33(9):1008–1019.
- Warburg O. [The effect of hydrogen peroxide on cancer cells and on embryonic cells]. *Acta Unio Int Contra Cancrum*. 1958;14(1):55–57. German [with English abstract].
- Pavlova NN, Thompson CB. The emerging hallmarks of cancer metabolism. *Cell Metab*. 2016;23(1):27–47.
- Masoud GN, Li W. HIF-1 $\alpha$  pathway: role, regulation and intervention for cancer therapy. *Acta Pharm Sin B*. 2015;5(5):378–389.
- Cavadas MA, Nguyen LK, Cheong A. Hypoxia-inducible factor (HIF) network: insights from mathematical models. *Cell Commun Signal*. 2013;11(1):42.
- Kang HG, Jenabi JM, Liu XF, Reynolds CP, Triche TJ, Sorensen PH. Inhibition of the insulin-like growth factor I receptor by epigallocatechin gallate blocks proliferation and induces the death of Ewing tumor cells. *Mol Cancer Ther*. 2010;9(5):1396–1407.
- Shimobayashi M, Hall MN. Making new contacts: the mTOR network in metabolism and signaling crosstalk. *Nat Rev Mol Cell Biol*. 2014;15(3):155–162.
- Casero RA Jr, Murray Stewart T, Pegg AE. Polyamine metabolism and cancer: treatments, challenges and opportunities. *Nat Rev Cancer*. 2018 Sep 4.
- Hudson CC, Liu M, Chiang GG, et al. Regulation of hypoxia-inducible factor 1 $\alpha$  expression and function by the mammalian target of rapamycin. *Mol Cell Biol*. 2002;22(20):7004–7014.
- Wolff NC, Vega-Rubin-de-Celis S, Xie XJ, Castrillon DH, Kabbani W, Brugarolas J. Cell-type-dependent regulation of mTORC1 by REDD1 and the tumor suppressors TSC1/TSC2 and LKB1 in response to hypoxia. *Mol Cell Biol*. 2011;31(9):1870–1884.
- Huang J, Manning BD. A complex interplay between Akt, TSC2 and the two mTOR complexes. *Biochem Soc Trans*. 2009;37(Pt 1):217–222.
- Groenewoud MJ, Zwartkruis FJ. Rheb and Rags come together at the lysosome to activate mTORC1. *Biochem Soc Trans*. 2013;41(4):951–955.
- Zimmers TA, Jin X, Hsiao EC, McGrath SA, Esquela AF, Koniaris LG. Growth differentiation factor-15/macrophage inhibitory cytokine-1 induction after kidney and lung injury. *Shock*. 2005;23(6):543–548.
- Jorgensen TJ, Tian H, Joseph IB, Menon K, Frost D. Chemosensitization and radiosensitization of human lung and colon cancers by antimetabolic agent, ABT-751, in athymic murine xenograft models of subcutaneous tumor growth. *Cancer Chemother Pharmacol*. 2007;59(6):725–732.
- Spolitu S, Uda S, Deligia S, Frau A, Collu M, Angius F, Batetta B. Multidrug resistance P-glycoprotein dampens SR-BI cholesterol uptake from high density lipoproteins in human leukemia cells. *Am J Cancer Res*. 2016;6(3):615–627.

27. Morin PJ. Drug resistance and the microenvironment: nature and nurture. *Drug Resist Updat*. 2003;6(4):169–172.
28. De Milito A, Canese R, Marino ML, et al. pH-dependent antitumor activity of proton pump inhibitors against human melanoma is mediated by inhibition of tumor acidity. *Int J Cancer*. 2010;127(1):207–219.
29. Longo DL, Bartoli A, Consolino L, et al. In vivo imaging of tumor metabolism and acidosis by combining PET and MRI-CEST pH imaging. *Cancer Res*. 2016;76(22):6463–6470.
30. Spugnini EP, Citro G, Fais S. Proton pump inhibitors as anti vacuolar ATPases drugs: a novel anticancer strategy. *J Exp Clin Cancer Res*. 2010;29:44.
31. Fais S, De Milito A, You H, Qin W. Targeting vacuolar H<sup>+</sup>-ATPases as a new strategy against cancer. *Cancer Res*. 2007;67(22):10627–10630.
32. Fais S. Proton pump inhibitor-induced tumour cell death by inhibition of a detoxification mechanism. *J Intern Med*. 2010;267(5):515–525.
33. Wang H, Jia XH, Chen JR, et al. HOXB4 knockdown reverses multidrug resistance of human myelogenous leukemia K562/ADM cells by downregulating P-gp, MRP1 and BCRP expression via PI3K/Akt signaling pathway. *Int J Oncol*. 2016;49(6):2529–2537.
34. Rafiee P, Theriot ME, Nelson VM, et al. Human esophageal microvascular endothelial cells respond to acidic pH stress by PI3K/AKT and p38 MAPK-regulated induction of Hsp70 and Hsp27. *Am J Physiol Cell Physiol*. 2006;291(5):C931–C945.
35. Moore T, Beltran L, Carbajal S, et al. Dietary energy balance modulates signaling through the Akt/mammalian target of rapamycin pathways in multiple epithelial tissues. *Cancer Prev Res (Phila)*. 2008;1(1):65–76.
36. Ching CB, Hansel DE. Expanding therapeutic targets in bladder cancer: the PI3K/Akt/mTOR pathway. *Lab Invest*. 2010;90(10):1406–1414.
37. Marhold M, Tomasich E, El-Gazzar A, et al. HIF1 $\alpha$  Regulates mTOR signaling and viability of prostate cancer stem cells. *Mol Cancer Res*. 2015;13(3):556–564.
38. Brown LM, Cowen RL, Debray C, et al. Reversing hypoxic cell chemoresistance in vitro using genetic and small molecule approaches targeting hypoxia inducible factor-1. *Mol Pharmacol*. 2006;69(2):411–418.
39. Unruh A, Ressel A, Mohamed HG, et al. The hypoxia-inducible factor-1 alpha is a negative factor for tumor therapy. *Oncogene*. 2003;22(21):3213–3220.
40. Rohwer N, Dame C, Haugstetter A, et al. Hypoxia-inducible factor 1alpha determines gastric cancer chemosensitivity via modulation of p53 and NF-kappaB. *PLoS One*. 2010;5(8):e12038.
41. Dan HC, Sun M, Yang L, et al. Phosphatidylinositol 3-kinase/Akt pathway regulates tuberous sclerosis tumor suppressor complex by phosphorylation of tuberlin. *J Biol Chem*. 2016;291(43):22848.
42. Manning BD, Tee AR, Logsdon MN, Blenis J, Cantley LC. Identification of the tuberous sclerosis complex-2 tumor suppressor gene product tuberlin as a target of the phosphoinositide 3-kinase/akt pathway. *Mol Cell*. 2002;10(1):151–162.
43. Inoki K, Li Y, Zhu T, Wu J, Guan KL. TSC2 is phosphorylated and inhibited by Akt and suppresses mTOR signalling. *Nat Cell Biol*. 2002;4(9):648–657.
44. Huang J, Manning BD. The TSC1-TSC2 complex: a molecular switchboard controlling cell growth. *Biochem J*. 2008;412(2):179–190.

## OncoTargets and Therapy

### Publish your work in this journal

OncoTargets and Therapy is an international, peer-reviewed, open access journal focusing on the pathological basis of all cancers, potential targets for therapy and treatment protocols employed to improve the management of cancer patients. The journal also focuses on the impact of management programs and new therapeutic agents and protocols on

Submit your manuscript here: <http://www.dovepress.com/oncotargets-and-therapy-journal>

patient perspectives such as quality of life, adherence and satisfaction. The manuscript management system is completely online and includes a very quick and fair peer-review system, which is all easy to use. Visit <http://www.dovepress.com/testimonials.php> to read real quotes from published authors.

Dovepress